8th International Symposium on Magnetic Bearing
August 26-28, 2002, Mito, Japan

A ROTOR-CONTROLLED MAGNETIC BEARING

H. Ming Chen
Foster-Miller Technologies, Albany, NY 12205 USA
mchen@fosmiltech.com

Thomas Walter
Foster-Miller Technologies, Albany, NY 12205 USA
twalter@fosmiltech.com

ABSTRACT
A blood pump rotor is supported by two passive radial bearings made of repulsive permanent-magnet (PM) rings. In one of the radial bearings, the rotor magnet ring is controlled to slide axially back and forth and achieve an active thrust bearing function. This innovative active thrust magnetic bearing concept requires on-rotor implementation of all electronics for control, displacement sensing, and power. This paper discusses the mechanism of the thrust bearing, the associated dynamics, and the control method. It also addresses on-rotor electrical power generation for operation of the electronics.

INTRODUCTION
Blood pumps with magnetic bearing rotors feature large bearing gaps and no mechanical contact seals, thus reducing the impact on blood hemolysis and clotting. The levitation of these rotors usually involves using a combination of passive and active magnetic bearings to control translatory and angular rotor motions [1]. Although passive bearings using PMs are simple, conventional active bearings that require sensors, electromagnetic actuators, and the associated electronics are too complicated and bulky, especially for small implantable blood pumps or ventricle assist devices (VADs). Further, an active magnetic bearing adds many electrical wires in additional to the motor driving wires, imposing a reliability burden. Increasing pump reliability involves reducing the wire count, and minimizing the number of active control axes.

The desire to make a magnetic bearing blood pump appear totally passive, so that it is less bulky with no bearing wires, prompted the idea presented herein. According to Earnshaw's law, however, at least one active axis is required to stabilize the magnetic levitation. This concept supports a VAD rotor with four passive axes and one active axis. The mechanical components and control electronics of the active axis are all mounted on the rotor and thus are transparent to the user.

Figure 1 presents a specific magnetic bearing configuration for a VAD (about 40 mm in diameter and 60 mm in length) with an axial or mixed-flow type of blood pump. As shown, the two passive radial bearings are made of axially polarized PM rings. One of the radial bearings has a controllable rotor PM ring, which can be made to slide axially for a small displacement, say ± 0.5 mm. By moving the PM ring back and forth according to feedback from a rotor-mounted axial displacement measurement, the rotor floats without touching the stators at either end. Therefore, this radial bearing also functions as the thrust bearing, which completes the requirement for total magnetic levitation of the rotor. This idea is similar to the one presented in reference [2], but more involved in that the control is installed inside the rotor. The pump's thrust control is discussed in the following, as well as the on-board generator design that provides electrical energy to power the actuator and rotor-mounted electronics.

MATHEMATICAL MODEL
The rotor is subjected to a negative axial stiffness at each passive radial bearing ($-K_m$). Although not necessary, assume for simplicity that the negative stiffnesses are identical. To enable the sliding rotor magnet to restore its location on rotor, the magnet is connected axially to the rotor by a spring and damper. A dithering axial control force is applied to the sliding magnet by using an onboard actuator to move the magnet back and forth and overcome the instability that results from the axial negative stiffnesses. Naturally, the force applied to the magnet is reacted by the rotor.

Mathematically, the rotor thrust dynamics can be represented by the following two equations:

$$M\frac{d^2X}{dt^2}+C(\frac{dX}{dt}-\frac{dX_1}{dt})+K(X-X_1)=-F+K_mX+F_t \quad (1)$$

$$m\frac{d^2X_1}{dt^2}+C(\frac{dX_1}{dt}-\frac{dX}{dt})+K(X_1-X)=F+K_mX_1 \quad (2)$$

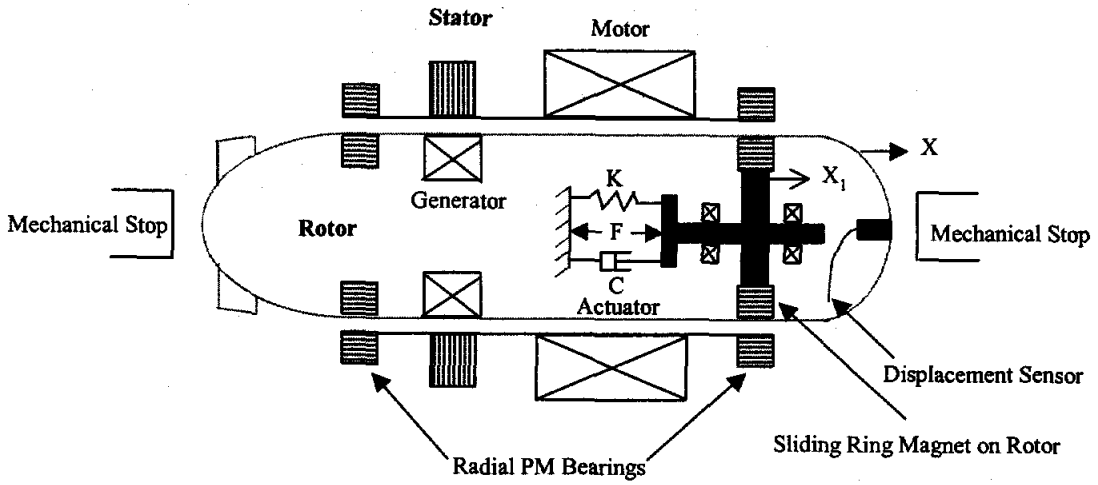

FIGURE 1: A rotor-controlled thrust bearing concept

where:

- M = rotor mass excluding sliding mass of magnet and its attachment
- m = sliding mass of magnet and its attachment
- X = rotor axial displacement
- X_1 = sliding magnet axial displacement
- K = axial stiffness coefficient of mechanical spring connecting sliding magnet to rotor
- C = axial damping coefficient of damper connecting sliding magnet to rotor
- K_m = axial stiffness coefficient per radial bearing (a positive number)
- F_t = thrust force on rotor
- F = dithering force
- t = time.

Given a possible combination of masses (M, m) and a negative axial stiffness at each radial bearing ($-K_m$), we have to determine a set of mechanical stiffness and damping coefficients (K, C) and a control law for the dithering force (F), to make the dynamic system stable. The simplest control law would be a proportional derivative (PD) feedback law as defined by:

$$F = C_p X + C_d \frac{dX}{dt} \qquad (3)$$

where:

- C_p = proportional constant
- C_d = derivative constant.

It is assumed that we will measure the rotor displacement (X) by using an onboard displacement sensor such as an eddy-current probe or a Hall-effect probe.

Taking and combining the Laplace transform of equations (1), (2) and (3), the following normalized system characteristic equation is obtained:

$$\mu S^4 + [(1+\mu)C + \mu C_d]S^3 + [(1+\mu)(K-1) + \mu C_p]S^2 - (2C + C_d)S + (1 - 2K - C_p) = 0 \qquad (4)$$

where:

- μ = m/M
- S = Laplace variable.

The parameters in equation (4) are normalized quantities [2] as defined below:

- $S \rightarrow S/B$
- $C \rightarrow C/\sqrt{MK_m}$
- $C_d \rightarrow C_d/\sqrt{MK_m}$
- $K \rightarrow K/K_m$
- $C_p \rightarrow C_p/K_m$

where:

- $\rightarrow$ = imply
- $B = \sqrt{K_m/M}$.

The artificial parameter B provides a calibration of the system natural frequency and how stiff the active thrust bearing can be made.

Stability Design Using Pole Placement Method

In equation (4), there are five parameters to be determined (μ, K, C, C_p and C_d) so that the system has stable roots in the left half of S-plane. Usually, the mass ratio μ is a given value, dictated by radial bearing size and other physical constraints. To achieve a stable dynamic system, we may assign desired stable roots into equation (4), for example, $-1 \pm j$ and $-2 \pm 2j$. The equivalent characteristic equation is thus:

$$(S+1+j)(S+1-j)(S+2+2j)(S+2-2j) = 0 \qquad (5)$$

Assuming $\mu = 0.1$ and comparing equations (4) and (5), the following four normalized system parameters are obtained: C = 0.933; K = 3.289; C_d = -4.263; C_p = -7.179.

Using the final value theorem, the normalized static stiffness of the active thrust bearing is:

$$K_{ax} = (1 - 2K - C_p)/(K-1) \qquad (6)$$
$$= 0.7 \text{ for the above case.}$$

For a rotor weight of 114 g and an axial stiffness of -1.75×10^4 N/m (-17.5 N/mm) per radial bearing, we have demonstrated the dynamic stability of the above system using a liftoff (from a mechnical stop at inlet end) transient simulation analysis. Under a thrust load of 0.875 N toward the inlet side, the displacements of the rotor (X) and sliding magnet (X_1) are presented in Figure 2. At the steady state, X = -0.73 mm and X_1 = 0.123 mm. Therefore, the sum of axial forces exerted on rotor by the two radial bearings is equal to:

(-0.073 + 0.123)(17.5) = 0.875 N = thrust load.

The rotor steady-state deflection under the thrust load can also be predicted by equation (6). In this case, the axial static stiffness of the control system is 0.7*17.5 or 12.3 N/mm, which thus confirms the rotor deflection to be:

X = -0.875/12.25 = -0.073 mm.

Figure 3 presents the required transient control force applied to the sliding magnet, which settles to a steady-state value of 9.14 N. However, in this equilibrium condition the radial bearings exert forces in opposite directions, and there is a waste of control energy in the actuator. The following section addresses this issue.

ZERO-FORCE SEEKING ALGORITHM

To minimize control energy, the PD control law (3) is modified by adding a force integral feedback, i.e.,

$$F = C_p(X - \delta) + C_d \frac{dX}{dt} \qquad (7)$$

where:

$$\delta = C_i \int_0^t F dt$$

C_i = integral constant.

Equation (7) imposes nonlinear relationships among the five parameters, including C_i. This makes the pole placement method difficult for use in deriving an appropriate value of the integral constant. We have determined it numerically to be $C_i = 0.144 \times 10^{-3}$ m/N-sec for the above case. With this integral control, the transient example was recalculated. The displacement results are shown in Figure 2, with the resulting control force shown in Figure 3.

With the integral control, the steady-state rotor and sliding magnet displacements are 0.021 mm and 0.030 mm, respectively. Apparently, both radial bearings now produce axial forces in the same direction to balance the thrust load of 0.875 N. Also with the integral control, the steady-state control force approaches zero. As a result, the control energy in the actuator will be minimized.

HARDWARE CONSIDERATIONS

The major elements in this magnetically levitated blood pump include the motor, radial bearings, generator,

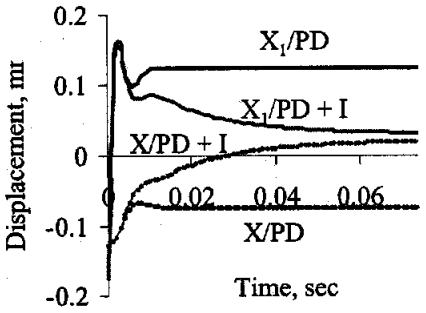

FIGURE 2: Liftoff transient displacements with and without integral control

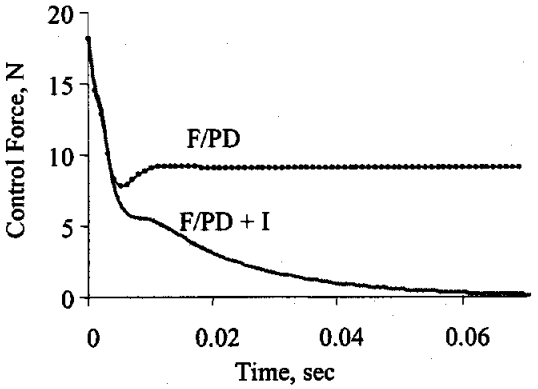

FIGURE 3: Liftoff transient actuator force with and without integral control

power electronics, force actuator, control electronics, and the displacement sensor and its conditioning electronics. The miniaturization of the control and sensing electronics on rotor is not seen as a problem, because they consume very little power.

Motor

An ironless brushless dc motor using a four-pole Halbach array [3] of NdFeB magnets has been designed and tested to deliver 10 W at 10,000 rpm [4]. The motor components are shown in Figure 4.

The 25-mm-long magnet array is mounted on the rotor with an inside diameter of 16 mm and an outside diameter of 25 mm. The stator windings spread in the volume from 27 to 38 mm in diameter. The ironless motor imposes no radial or axial side pulls and is appropriate for passive radial bearing applications.

Radial Bearings

Two radial bearings with identical PM components have been sized for this pump. Each bearing has a stator PM ring and a rotor PM ring with the same cross section of 4 by 4 mm. The rotor ring outer diameter is 23.8 mm, and the stator ring inner diameter is 27 mm. Both rings are made of NdFeB and axially polarized to a remnant flux density of 1.2 T. The calculated radial stiffness is about 8750 N/m per bearing. Doubling this value yields the axial (unstable) stiffness, considering there is no ferromagnetic material nearby.

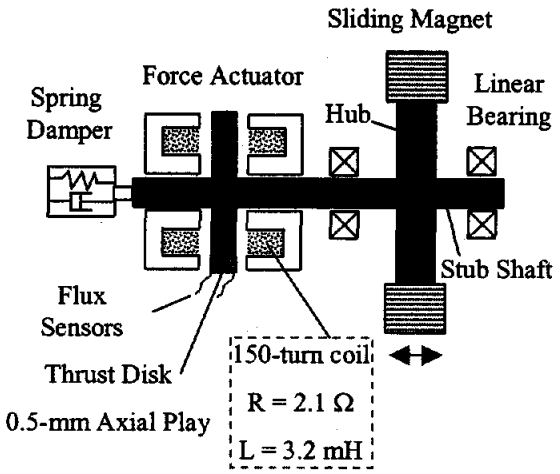

FIGURE 4: Dithering control mechanism

Force Actuator

The rotor PM ring of one radial bearing is fixed to a circular hub at its inner diameter; it is free at its outer diameter as illustrated in Figure 5. A small stub shaft goes through and is attached to the hub center. The stub shaft is supported by two linear bearings, and it is free to slide back and forth axially. A conventional thrust-magnetic-bearing-like electromagnetic device is used to drive the stub shaft and the sliding magnet. A thrust disk is mounted on the shaft, and two stators, each with a coil, are at each side of the disk. Hall-effect probes measure the flux density to indicate magnetic forces in the air gaps. This force actuator acts as a dither control and is designed with low inductance, so that it produces actuating force much faster than the controlled system can respond. To produce a required force, only one stator coil is energized by a dc source using a bang-bang control with hysteresis. Figure 6 presents a typical fast current response in the stator coil. The delay of about 1 msec of current (thus the force output of the actuator) is insignificant to the much slower thrust control. In practice, part of the actuator may be tucked inside of the motor Halbach array.

Generator and Power Electronics

With the zero-force-seeking ability described above, thrust control power should be low, as it will only be needed for the electronics circuitry and occasionally to control rotor disturbance. However, the size of the generator and thus the power electronics is dictated by the peak load requirement. For example, Figure 3 shows the thrust control requires an initial peak force of 18 N. Although it is only needed for a small period of time, the rotor cannot lift off without this force capacity. This 18-N peak force value is twice as large as what the force actuator can deliver.

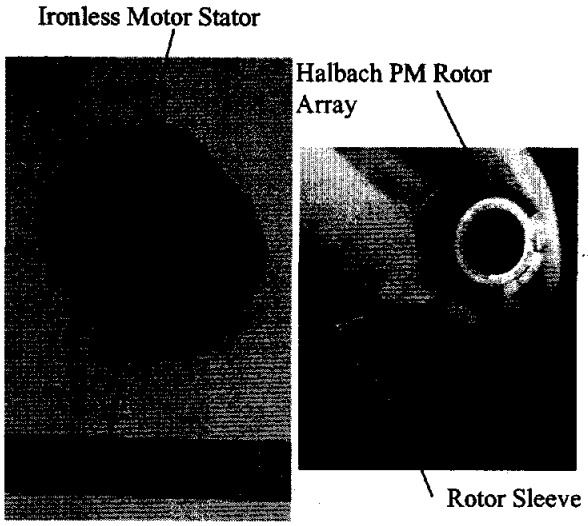

FIGURE 5: Ironless motor components

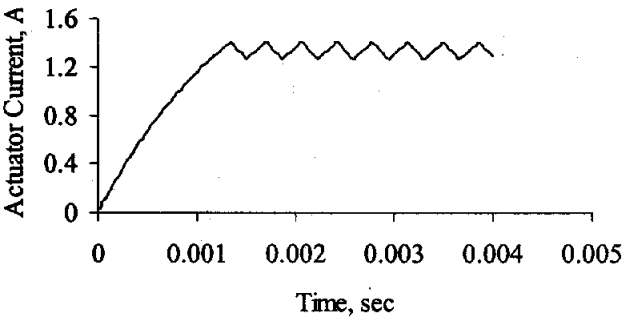

FIGURE 6: Actuator current response under a bang-bang voltage control with hysteresis

To reduce this force requirement, the dynamic system is made softer by choosing the system roots. For example, -0.5 ± 0.5j and -1 ± j, with the corresponding parameters: C = 0.367; K = 1.622; C_p = -2.344; C_d = -1.033, for μ = 0.1. The transient responses were recalculated and are presented in Figures 7 and 8. Figure 8 indicates a peak force of 4.45 N, which is within the capacity of the above actuator using a current of 1.34 A (see Figure 6). With this actuator current requirement and its resistance and inductance, we can devise a suitable generator.

A pulse-type generator similar to a switched reluctance machine was presented in [5]. It effectively uses copper wire to generate high frequency voltage pulses, which can be rectified and smoothed using a small capacitor. However, it has a large negative radial stiffness due to PM flux bias, which has to be compensated by using stronger radial bearings. To circumvent the side-pull problem, we choose an ironless generator using a dipole Halbach array [6] on the stator using eight magnets, and three phases of copper wires on the rotor as shown in Figure 9.

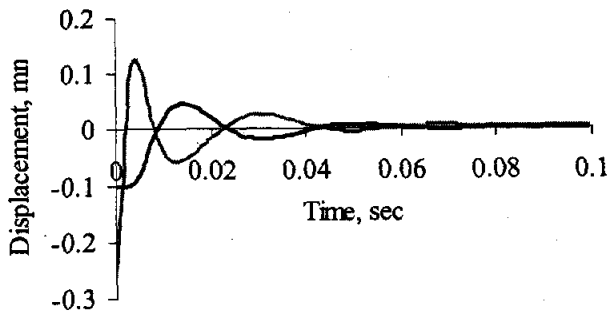

FIGURE 7: Liftoff transient displacements for a softer axial system

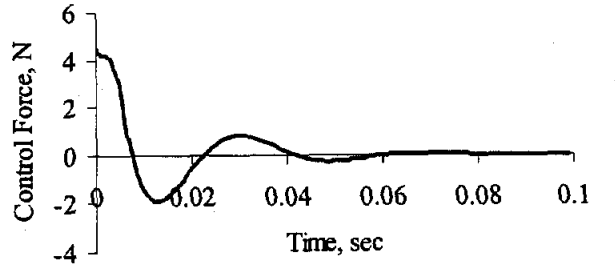

FIGURE 8: Liftoff transient actuator for a softer axial system

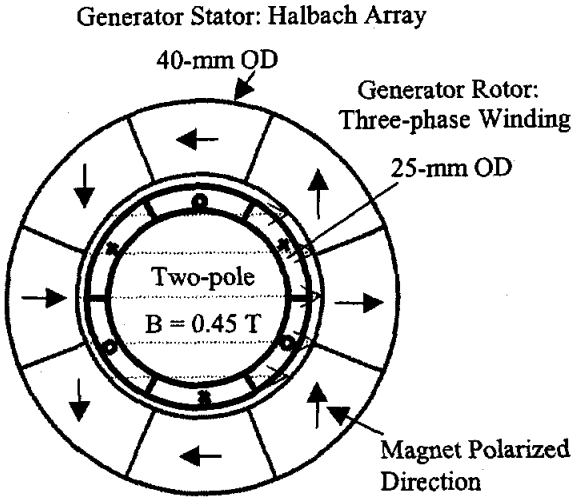

FIGURE 9: Two-pole ironless generator

The dipole flux is confined within the array, and the flux density was calculated to 0.45 T. Each phase employs 200 coil turns of 0.5-mm-thick copper wire. The coil has an average diameter of 20 mm and an effective conductor length of 10 mm. The phase resistance is estimated to be 1.0 Ω. Each phase produces a peak voltage of 5.5 V at 3000 rpm.

A three-phase full-wave rectifier circuit [7] can be applied to the generator output. The rectified output at 5.5 V has minimal ripple content. It can directly power the force actuator with no need of smoothing. The output smoothing at such a low frequency and low voltage would require a capacitor too large for the rotor to accommodate. The same rectified output will be further regulated to power the electronic control circuitry.

It should be noted that the rotor is initially supported in the axial direction on a mechanical stop. At 3,000 rpm, the generator output voltage is high enough to power the electronics and force actuator, and the rotor will lift off the stop.

CONCLUSIONS

An innovative concept has been presented for implementation of a thrust magnetic bearing control on a blood pump rotor supported by passive radial bearings. The concept involves dithering a radial bearing magnet axially to overcome the negative axial stiffness of the radial bearings. To prove concept feasibility, we have achieved the following:

1. The thrust-bearing-controlled dynamics was modeled as a system with two degrees of freedom using a PD displacement feedback controller to generate the dithering force. It has been shown that stable systems can be designed with different PD gains and magnet-to-rotor attachments (mechanical spring and damper) using a pole-placement method.
2. A zero-force-seeking ability involving a control force integral was added to the PD controller. The modified control eliminates the dc control force and thus the actuator dc coil current. This minimizes the power consumption of the active thrust control.
3. A force actuator (similar to a conventional thrust magnetic bearing) with 5-N peak-force capacity and a short time constant was sized to fit the small rotor application.
4. An ironless two-pole three-phase generator was sized to harness rotor rotational power (provided by a four-pole ironless brushless dc motor) and produce electrical power on the rotor. To avoid the use of large capacitors, the generator output was rectified but not filtered for powering the actuator with a bang-bang scheme. Also, the output was voltage clamped using Zener diodes before powering the control electronics.

A prototype of the blood pump is being developed. The initial test plan calls for a "non-rotating" or a stationary rotor to enable proof of concept and allow measurement of mechanical and electrical parameters without the added complexity of rotation. The two-pole generator stator will be rotated in the initial tests to produce electrical power on rotor.

ACKNOWLEDGMENTS

The authors express gratitude to colleague Nga Lee for consultation on integrated circuitry and power electronics. They also thank Foster-Miller Technologies for the permission to publish this study.

REFERENCES

1. Chen, H. Ming, et al. "Development of Magnetically Levitated Blood Pumps." Presented at 6th International Symposium on Magnetic Suspension Technology, Turin, Italy, October 7-11, 2001.
2. Chen, H. Ming. "A Stator-Controlled Magnetic Bearing." Presented at 6th International Symposium on Magnetic Bearings, August 5-7, 1998, Cambridge, MA.
3. Halbach, K. "Design of Permanent Multipole Magnets with Oriented Rare Earth Cobalt Material." *Nuclear Instruments and Methods*, Vol. 169, 1980, North Holland Publishing Co.
4. Chen, H. Ming. "High-Efficiency Rotary Blood Pump." Phase I SBIR Final Report prepared for National Institutes of Health, October 2001.
5. Chen, H. Ming and T. Walter. "A Self-Sufficient Magnetic Bearing. " Presented at 6th International Symposium on Magnetic Suspension Technology, Turin, Italy, October 7-11, 2001.
6. Johnson, D., et al. "High Speed PM Motor with Hybrid Magnetic Bearing for Kinetic Energy Storage." Proceedings of 2001 IEEE Industry Applications Society 36th Annul Meeting – IAS'01, Chicago, IL, September 30 – October 4, 2001.
7. Kenjo, T. *Power Electronics for the Microprocessor Age*. Oxford University Press Inc., New York, 1994.